

The Detection of Lung Tumors Using CT scan Images with Feature Extraction and Segmentation Techniques.

Ms. Seema B. Rathod¹, Dr. Lata L. Ragha²

Submitted: 28/08/2023

Revised: 19/10/2023

Accepted: 01/11/2023

Abstract: In this paper, we present a comparative study of segmentation and feature extraction techniques for lung cancer detection. Various segmentation techniques, including Thresholding, global Thresholding, and watershed segmentation, are performed and evaluated. Additionally, feature extraction is conducted to further enhance the performance of segmentation techniques. The proposed approach is compared with existing techniques to highlight its effectiveness and potential for improved lung tumor detection. In this research work, we analyse two tables: the first presents textual-based results, and the second provides statistical values. Unlike the existing system that employs only one technique, we apply different techniques on 5 images for analysis. The results demonstrate that the proposed segmentation and feature extraction techniques can achieve higher accuracy and potentially aid in early lung cancer detection.

Keyword: Artificial Intelligence, pattern recognition, Segmentation, Medical Images, K-means, Edge-Based, Thresholding, Feature extraction.

1. Introduction

Various nations have evaluated systems for lung tumor detection, as the majority of people on Earth face the risk of this deadly cancer, leading to fatalities.[1] The NLST evaluation revealed that existing low-quality CT scan images were used, resulting in lower accuracy, and radiologists had to deal with a large number of CT scan images as a consequence of these procedures.[2] Due to the challenging nature of identifying lesions, even experienced physicians may find it difficult to visualize them. Consequently, the workload on radiologists significantly escalates when they have to analyse a larger number of CT images [3] In 2008, a total of 356 Jordanians were diagnosed with lung cancer, accounting for 7.7% of all newly reported cases. The ratio of male to female lung cancer cases was 5:1, with 297 (13.1%) men and 59 (2.5%) women. Among men, lung cancer ranked second in terms of the prevalence, while it ranked tenth among women. [4-5] As breast, colon, and prostate cancers continue to increase, they contribute to a significant number of deaths. Lung cancer alone accounts for approximately 170,000 excess deaths and 180,000 new cases annually, resulting in about 480 daily diagnoses and

460 deaths (Tina, 2005).[6] The global climate and pollution have resulted in millions of lives lost and increased cancer cases. This poses a significant challenge in the 21st century, as stated by the World Health Organization (Tina, 2005)[7,8] After pre-processing, the focus of this discussion is on how segmentation and feature extraction assist in lung cancer diagnosis, including the description of feature categories and extraction methods. The natality wise display lung tumor is shown in Fig. 1.

Research Scholar Lokmanya Tilak College of Engineering Navi Mumbai University, India¹

Fr. C. Rodrigues Institute of Technology, India Navi Mumbai University, India.²

omseemarathod@gmail.com¹ lata.ragha@fcrit.ac.in²

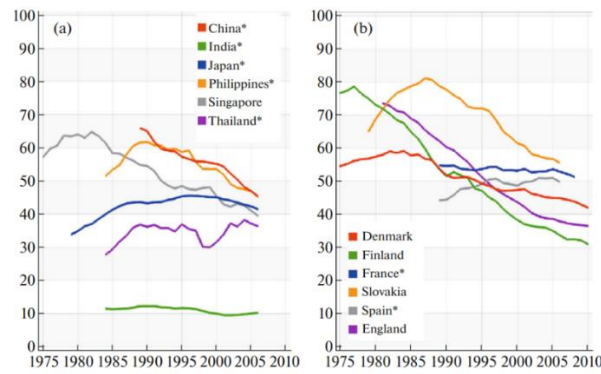


Fig.1 Natality wise define the lungs tumor for woman and man

2. Literature Survey

This paper presents diagnostic technical materials and identifies various computer-aided detection (CAD) systems for lung tumor detection (Mahersia, 2015).[9] In clinical practice, various radiation techniques are employed for tumor delineation. In this research, SUV thresholding was frequently utilized to accurately locate and determine the size of primary lung lesions and metastatic tumors. The predetermined SUV threshold values ranged from 36% to 44% using a SUV generator.[10] Nowadays, there are numerous tools available for the detection and prediction of lung tumors. These tools analyse CT scan images and mark any identified tumors. All of these tasks are performed by the computer-assisted system.[11] This paper employs machine learning and deep learning techniques with various hidden layers to improve the precision and accuracy of lung tumor classification or diagnosis using CT scan images. The approach involves training and testing to enhance prediction capabilities.[12] In this research, the median filter was utilized to average the pixel values in the targeted area, preserving edge locations and shapes. However, this approach may result in a reduction of some data that is relevant to CT scan images.[13-16] Artificial neural networks were employed to develop a computer-aided system for lung CT scan images. Morphological methods were utilized for lung segmentation, and Otsu's method was applied to convert the images into pixels. The classification process involved the utilization of statistical evaluation parameters by the author.[17] Artificial neural networks were employed to develop a computer-aided system for lung CT scan images. Morphological methods were utilized for lung segmentation, and Otsu's method was applied to convert the images into pixels. The classification process involved the utilization of statistical evaluation parameters by the author.[18] The authors employed the CNN algorithm to diagnose lung cancer using X-ray images. They utilized the CC-net model, which incorporates a criss-cross attention component, for effective classification.[19,20] A deep learning-based model, called Robotic, was utilized

for lung tumor segmentation using CT scan images as input. Additionally, X-ray images were employed for the segmentation network of lung images.[21] The method proposed by [22] utilizes tissue, shape, and D approach to identify lung nodules, incorporating features such as surface identification, Fourier shape analysis, and CNNs. In contrast, [23] focuses on computer-aided diagnostics (CAD) with physically constructed models.

Research Work's Contribution

1. For the purpose of early lung cancer diagnosis utilising CT scan pictures, a unique here use different segmentation techniques for correct direction images. finding some statical value after training on LIDC datasets.
2. The suggested architecture includes transfer learning for feature extraction and enhanced segmentation using the capsule network. The high diagnostic rate can also be increased by the suggested fusion algorithm.
3. The whale optimization approach is suggested for developing the saliency map and service module network composite features. and from the results defined a best segmentation technique for analysis lung tumor using CT scan Images.

3. Material and Mythology

Dataset: In the implementation phase, a dataset of real patient CT scan images was collected from a lung image dataset that specifically focuses on lung cancer. This dataset contains CT scan images of the chest with annotations regarding lung nodules and tumors. The LIDC dataset comprises 1018 cases collected from seven different centres and 5 medical imaging institutes. The images are in DICOM format with a pixel size of 512 x 512. To facilitate evaluation, the DICOM images were converted to grayscale JPEG images using microDicom software. The proposed model was developed using Python programming language and executed using the Co-Lab online lab provided by Google, which allows

researchers to run machine learning programs online for free.

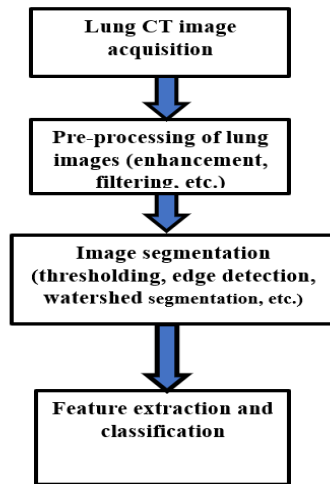


Fig. 2 Depicts a flow diagram of lung cancer detection.

and those without. A total of 1018 CT scan images were used for classification, employing 5-fold cross-validation to prevent overfitting. The classification model was trained on a combination of 20 DICOM images from the LIDC database, and the results were validated using 5 images containing a total of 19 nodules.

During implementation, the following challenges were encountered:

- The large size of the database posed difficulties in downloading.

- Understanding the structure of the database, defined in an XML file, presented challenges.

In this model, the first step is pre-processing. During pre-processing, the Wiener filter and Canny edge filter are applied to clean images and remove noise. The evaluation of these filters was discussed previously, utilizing parameters like PSNR, MSR, and RMS [30] to determine effectiveness and compare results.

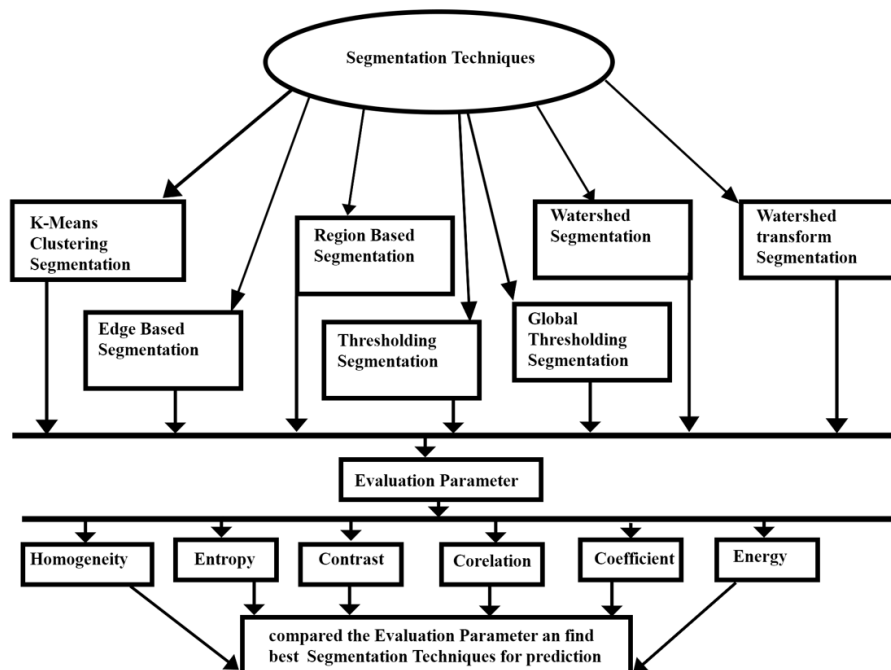


Fig. 3 Segmentation Techniques for Evaluation on CT Scan Images

The next step is segmentation, employing various segmentation techniques to analyse CT scan images.

Images are divided into subparts for analysis using methods like K-means Clustering, Edge-Based, Region

Based, Global Thresholding, Watershed, and Watershed Transform. After segmentation, feature extraction is performed to identify lung tumors. Mathematical functions are used for tumor detection, and a total of 5 images are used for segmentation and feature extraction.

As shown in following fig.4 display some analysis the tumor using segmentation techniques

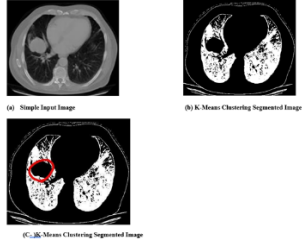
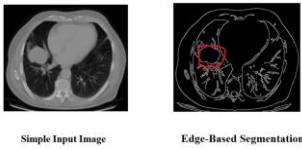
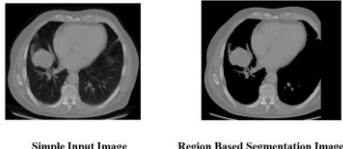
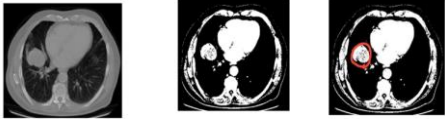

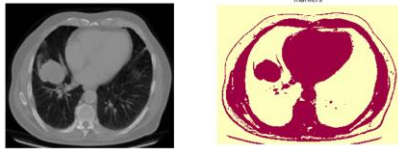
Segmentation Techniques	After segmentation techniques images
K-means Clustering	 <p>(a) Simple Input Image (b) K-Means Clustering Segmented Image (c) K-Means Clustering Segmented Image</p>
Edge-Based	 <p>Simple Input Image Edge-Based Segmentation Image</p>
Region Based	 <p>Simple Input Image Region Based Segmentation Image</p>
Global Thresholding	
Watershed	
Watershed Transform	 <p>markers</p>

Fig. 4 Analysis the tumor using segmentation techniques

Feature extraction:

Texture features based on Gray Level Co-occurrence Matrix (GLCM) are statistical measures utilized to describe image in texture. The GLCM matrix represents the frequency of pixel value pairs at a specific distance

and direction. Common texture features include contrast, energy, homogeneity, entropy, and correlation. Mathematical equations commonly used to compute these texture features in the results section are presented below. As shown following parameter are used for analysis the results. All Parameter Given in mathematics Equation

Contrast:

$$C = \sum_j^i [(i - j)^2 * p(i, j)] \quad \text{Eq. (1)}$$

Energy

$$E = \sum_j^i p(i, j)^2 \quad \text{Eq. (2)}$$

Homogeneity

$$H = \sum_j^i [p(i, j) / (1 + |i - j|)] \quad \text{Eq. (3)}$$

Entropy:

$$H = - \sum_j^i (p(i, j) * \log_2(p(i, j))) \quad \text{Eq. (4)}$$

Correlation:

$$r = \frac{(n \sum xy - \sum x)(n \sum y - (\sum y)^2)}{\sqrt{(n \sum x^2 - (\sum X)^2) * (n \sum y^2 - (\sum y)^2)}} \quad \text{Eq. (5)}$$

Statistical parameters are quantitative measures that describe the characteristics of a data set. Some common statistical parameters include:

Mean:

$$\mu = (x_1 + x_2 + \dots + x_n) / n \quad \text{Eq.(6)}$$

Median:

$$\text{Median} = (n + 1) / 2 \text{th value} \quad \text{Eq. (7)}$$

Standard deviation:

$$\sigma = \sqrt{\sum (x - \mu)^2 / n} \quad \text{Eq.8}$$

$$\text{Skewness: skewness} = [n / ((n - 1) * (n - 2))] * \sum ((x_i - \bar{x})^3) / s^3 \quad \text{Eq.(9)}$$

Kurtosis:

$$\text{kurtosis} = [n * \sum ((x_i - \bar{x})^4) / (s^4 * (n - 1))] - [3 * (n - 1)^2 / ((n - 2) * (n - 3))] \quad \text{Eq. (10)}$$

Fifth and sixth central moment:

$$\mu_5 = E[(X - \mu)^5] \quad \text{Eq. (11)}$$

$$\mu_6 = E[(X - \mu)^6] \quad \text{Eq. (12)}$$

3. Results and Discussion

In equations 1 to 5, texture values are calculated on 5 CT scan images that are M1,M2,M3,M4 and M5. Texture values are analysed, and Watershed Segmentation is found to be the most effective for segmentation. After

segmentation, statistical values are extracted using equations 6 to 12 in the feature extraction process. Here we have also display in table 1 and Table 2 With graphical format. As shown in table we are analysis 5 images for results.

Table1: showing the texture feature values

Images	Segmentation Techniques	Homogeneity	Entropy	Contrast	Correlation coefficient	Energy
M1	K-Means lustering segmentation	0.936635	0.266205	0.139362	0.78525	7.739132
	EdgeBased Segmentation	0.908151	0.271121	0.160410	0.0437199	9.201833

	Region Based K=2 Segmentation	0.708740827	0.2711215	0.04400882	0.934174534	0.18172
	Global Thresholding Segmentation	0.9543247169	2.240182288	0.1234200330	0.8176292	5.9081721
	Thresholding Segmentation	0.957831900	0.3506707	0.04041222	0.93404480	1.29647
	Watershed Segmentation	0.964482	0.23859695	0.036529789	0.9973929	0.60448
	Watershed Transform Segmentation	0.9544362	0.8022876	0.11453854	0.6745935	2.756547
M2	K-Means lustering segmentation	0.936635	0.316205	0.439362	0.78525	6.839132
	EdgeBased Segmentation	0.728151	0.271121	0.160410	0.0437199	9.201833
	Region Based K=2 Segmentation	0.688740827	0.2711215	0.4400882	0.934174534	0.18172
	Global Thresholding Segmentation	0.7843247169	2.240182288	0.2234200330	0.8176292	5.9081721
	Thresholding Segmentation	0.887831900	0.3506707	0.34041222	0.93404480	1.29647
	Watershed Segmentation	0.964482	0.23859695	0.036529789	0.9939299	0.60448
	Watershed Transform Segmentation	0.90544362	0.8022876	0.51453854	0.6745935	2.756547
M3	K-Means lustering segmentation	0.916635	0.316205	0.339362	0.78525	6.839132
	EdgeBased Segmentation	0.858151	0.251121	0.460410	0.0437199	9.201833
	Region Based K=2 Segmentation	0.878740827	0.22611215	0.24400882	0.934174534	0.18172
	Global Thresholding Segmentation	0.8843247169	2.280182288	0.2234200330	0.8176292	5.9081721
	Thresholding Segmentation	0.787831900	0.3706707	0.34041222	0.93404480	1.29647
	Watershed Segmentation	0.964482	0.23859695	0.036529789	0.9939299	0.60448
	Watershed Transform Segmentation	0.9544362	0.4022876	0.31453854	0.6745935	2.756547
M4	K-Means lustering segmentation	0.826635	0.516205	0.239362	0.78525	6.839132
	Edge Based Segmentation	0.8728151	0.471121	0.360410	0.0437199	9.201833
	Region Based K=2 Segmentation	0.788740827	0.4311215	0.64400882	0.934174534	0.18172

	Global Thresholding Segmentation	0.8643247169	2.340182288	0.5234200330	0.8176292	5.9081721
	Thresholding Segmentation	0.897831900	0.3606707	0.54041222	0.93404480	1.29647
	Watershed Segmentation	0.964482	0.23859695	0.036529789	0.773929	0.60448
	Watershed Transform Segmentation	0.9044362	0.8022876	0.12453854	0.6745935	2.756547
M5	K-Means clustering segmentation	0.926635	0.316205	0.139362	0.78525	6.839132
	EdgeBased Segmentation	0.928151	0.271121	0.160410	0.0437199	9.201833
	Region Based K=2 Segmentation	0.778740827	0.2711215	0.04400882	0.934174534	0.18172
	Global Thresholding Segmentation	0.9543247169	2.240182288	0.1234200330	0.8176292	5.9081721
	Thresholding Segmentation	0.857831900	0.3506707	0.04041222	0.93404480	1.29647
	Watershed Segmentation	0.964482	0.23859695	0.036529789	0.993929	0.60448
	Watershed Transform Segmentation	0.9044362	0.8022876	0.11453854	0.6745935	2.756547

The provided data is a Table1: showing the texture feature values format that presents the performance metrics of various image segmentation techniques across different cases (M1, M2, M3, M4, M5). The metrics evaluated for these techniques include:

Homogeneity: A measure of how uniform the regions in the segmented image are. Higher values indicate more uniform regions.

Entropy: A measure of the randomness or disorder in the segmented image. Lower values indicate less randomness.

Contrast: A measure of the difference in intensity between the segmented regions. Higher values indicate greater contrast.

Correlation Coefficient: A measure of the linear correlation between the intensity values in the segmented

image. A value close to 1 indicates a strong positive correlation.

Energy: A measure of the overall energy or intensity distribution in the segmented image.

For each case (M1, M2, M3, M4, M5), different image segmentation techniques are applied, and the corresponding values for each metric are provided. These values represent the performance of each technique for the specific case and metric.

This data is useful for evaluating and comparing the performance of different image segmentation techniques in various scenarios, with a focus on the specified metrics. It helps in understanding how these techniques perform in terms of homogeneity, entropy, contrast, correlation coefficient, and energy for each case.

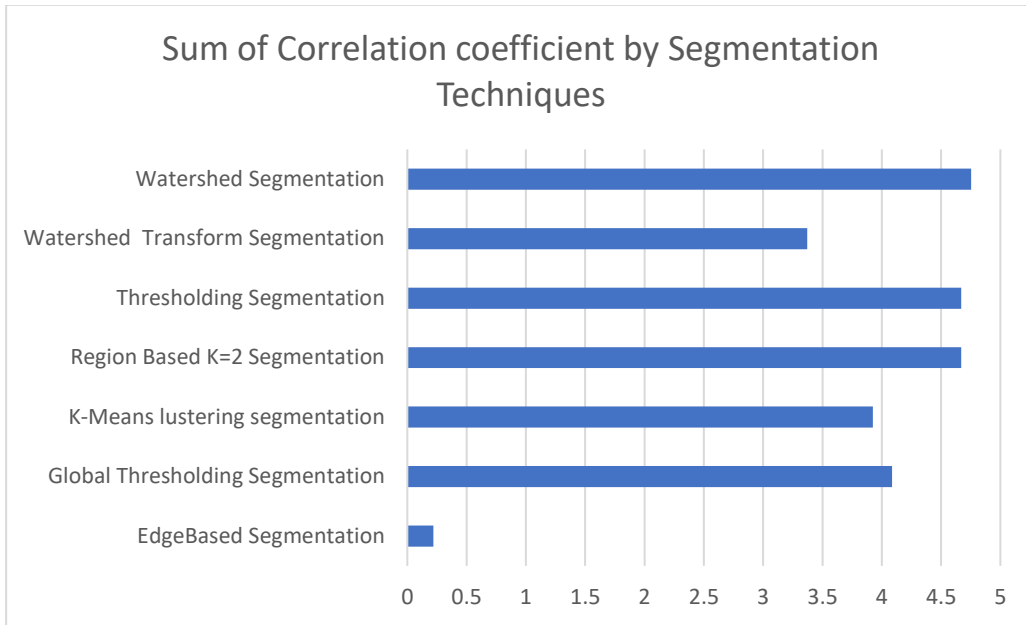


Fig. 5 Sum of Correlation coefficient watershed segmentation best

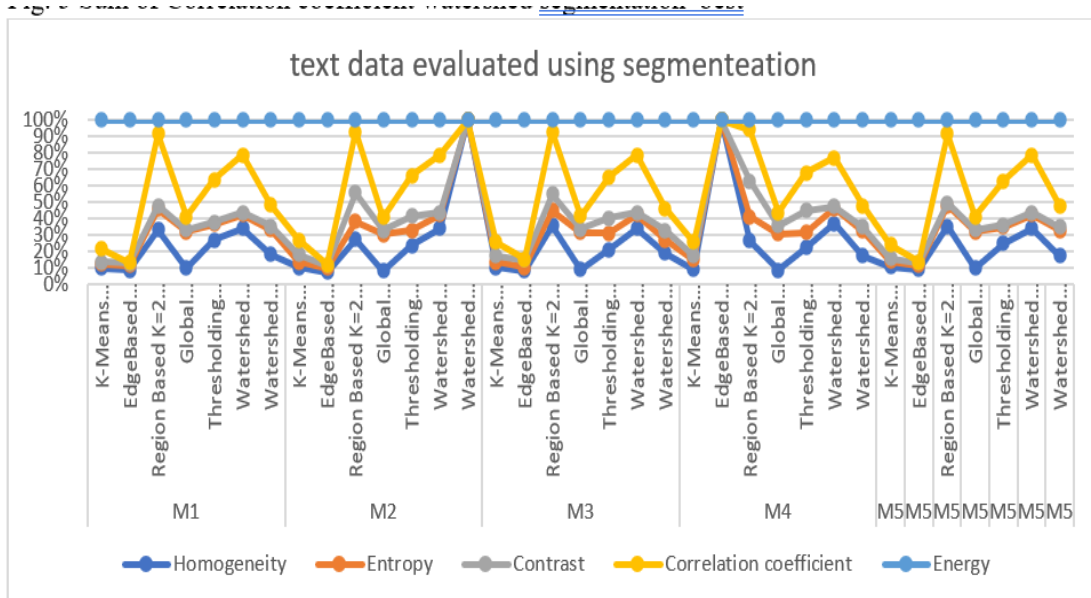


Fig. 6 Analysis the texture feature values

Table2: Table showing the statistical feature values

Images	Segmentation Techniques	Mean	S.D	Skewness	Kurtosis	FCM	SCM
M1	K-Means lustering segmentation	292	70.15	-1.177	2.906	-12.4	23.76
M1	EdgeBased Segmentation	223	53.10	-0.1897	1.010	-4.39	6.797
M2	Region Based K=2 Segmentation	262.94	62.66	-0.3893	1.848	-6.82	11.518
M2	Global Thresholding	291.43	29.79	-2.5778	8.606	-96.1	27.383

	Segmentation						
M3	Thresholding Segmentation	329.83	30.90	-0.5834	4.606	-2.78	8.9285
M4	Watershed Segmentation	341.58	125.5	-0.7305	4.809	-28.2	63.2674
M5	Watershed Transform Segmentation	328.76	123.7	-0.3819	1.713	-4.63	7.2373

The provided Table 2 contains information related to image segmentation techniques and their statistical characteristics. Here's a brief explanation of the data:

Images: Refers to different images or datasets under consideration.

Segmentation Techniques: Describes the various methods used for dividing or segmenting an image into distinct regions or **objects**. **Mean:** Represents the average value of a particular metric (e.g., pixel intensity) in the segmented regions' (Standard Deviation): Indicates the measure of the amount of variation or dispersion in the segmented regions.

Skewness: Measures the asymmetry or lack of symmetry in the distribution of values in the segmented regions. A negative skewness indicates a long tail on the left side.

mentioned statistical characteristics, such as mean, standard deviation, skewness, and kurtosis. The choice of technique and the specific values reported can help in

Kurtosis: Measures the tail ends or flatness of the distribution of values in the segmented regions. A positive kurtosis indicates heavy tails or outliers.

FCM (Fuzzy C-Means): A clustering algorithm that partitions data into clusters, providing information about the degree of membership of data points in each cluster's (Sugeno Fuzzy C-Means): Another variant of fuzzy clustering, which assigns hard (non-fuzzy) memberships to data points in clusters.

M1, M2, M3, M4, M5: These labels likely correspond to different models, datasets, or scenarios, and the statistics are reported for each. The Table 2 provides insights into how these different segmentation techniques perform based on the

evaluating and comparing these techniques for image segmentation tasks.

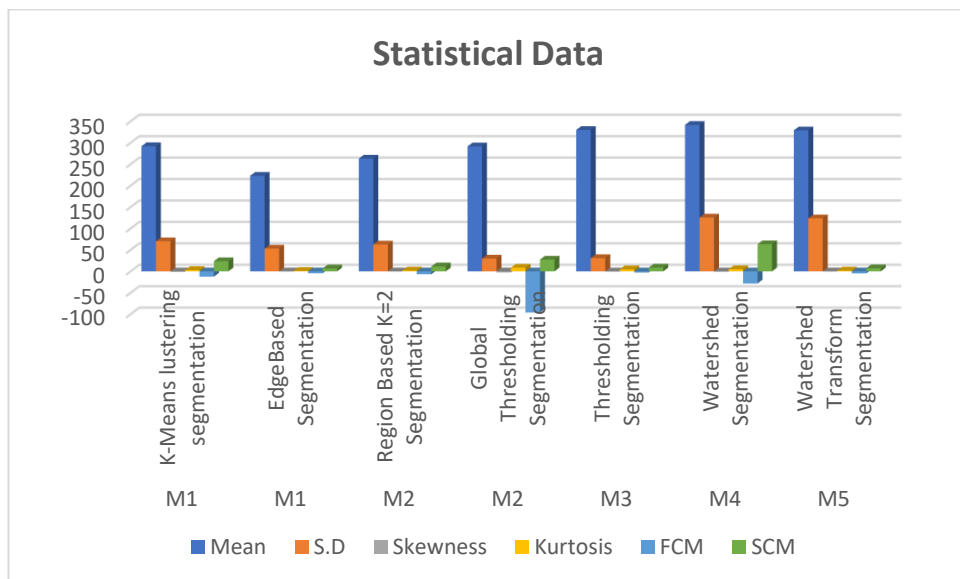


Fig. 7 Graph on Statistical Data

The above tables depict a system that employs 7 segmentation techniques to analyse lung tumors. Texture-based features are determined using GLCM at varying offset values. Energy, homogeneity, contrast, and

correlation are among the features calculated, which describe non-constant image values and skewness describes the variation in the ROI in statistical parameters.

4. Conclusion and Future work

The current paper elaborates extensively on the proposed technique for lung nodule detection, including the detection of the nodule itself and the computation of various features. The next step involves the potential for classifying regions of interest, which could be achieved using different types of classifiers.

Competing interests

The authors declare that they have no competing interests.

Consent for publication

Not applicable.

Ethics approval and consent to participate.

Not applicable.

Funding

This work is not Funding

Author's Contributions











Both authors read and approved the final manuscript.

References

- [1] Bharati S, Podder P, Mondal R, Mahmood A, Raihan-Al-Masud M. Comparative Performance Analysis of Different Classification Algorithm for the Purpose of Prediction of Lung Cancer. In: International Conference on Intelligent Systems Design and Applications. Vellore, India: Springer (2018). p. 447–57.
- [2] Coudray N, Ocampo PS, Sakellaropoulos T, Narula N, Snuderl M, Fenyo D, et al. Classification and Mutation Prediction From non–Small Cell Lung Cancer Histopathology Images Using Deep learning. *Nat Med* (2018) 24:1559–67. doi: 10.1038/s41591-018-0177-5
- [3] Nie L, Wang M, Zhang L, Yan S, Zhang B, Chua TS. Disease Inference from Health-Related Questions via Sparse Deep Learning. In: *IEEE Transactions on Knowledge and Data Engineering* (2015). p. 2107–19.
- [4] Smys, S., and Joy Iong-Zong Chen. "Special Section on Innovative Engineering Solutions for Future Health Care Informatics." *Journal of Medical Imaging and Health Informatics* 6, no. 7, pp. 1570-1571, 2016
- [5] Chandy, A., "A REVIEW on IOT based medical imaging technology for healthcare applications", *Journal of Innovative Image Processing (JIIP)*, 1(01), pp. 51-60, 2019.
- [6] Gajanand Gupta, "Algorithm for Image Processing Using Improved Median Filter and Comparison of Mean, Median and Improved Median Filter" *International Journal of Soft Computing and Engineering (IJSCE)* ISSN: 2231-2307, Volume-1, Issue-5, November 2011
- [7] H. Mahersia, M.Zaroug and Gabrella, "Lung Cancer Detection on CT Images: A Review on the Analysis Techniques" *International Journal of Advanced Research in Artificial Intelligence*, Vol.4, No.4,2015
- [8] S. Diederich, M. Thomas, M. Semik, H. Lenzen, N. Roos, A. Weber, W. Heindel, and D. Wormanns, "Screening for early lung cancer with low-dose spiral computed tomography: results of annual follow-up examinations in asymptomatic smokers," *Eur. Radiol.* 14 (4), 691–702.
- [9] Rathod, S., Ragha, L.: Using Weakly Supervised Machine learning Algorithms for Classification and Analysis of CT Scan Lung Cancer Images (2022)
- [10] Erdi, E. Yusuf, et al. "Segmentation of lung lesion volume by adaptive positron emission tomography image thresholding", *Cancer*, 80.S12, pp. 2505-2509, 1997.
- [11] S. Xie, Z. Yu, and Z. Lv, "Multi-disease prediction based on deep learning: a survey," *Computer Modeling in Engineering & Sciences*, vol. 128, no. 2, pp. 489–522, 2021.
- [12] T. Higaki, Y. Nakamura, J. Zhou et al., "Deep learning reconstruction at CT: phantom study of the image characteristics," *Academic Radiology*, vol. 27, no. 1, pp. 82–87, 2020.
- [13] X. P. Wang, B. Wang, P. Hou, and J. B. Gao, "Screening and comparison of polychromatic and monochromatic image reconstruction of abdominal arterial energy spectrum CT," *Journal of Biological Regulators & Homeostatic Agents*, vol. 31, no. 1, pp. 189–194, 2017.
- [14] Z. Wang, Y. Ni, Y. Zhang, Q. Xia, and H. Wang, "Laparoscopic varicocele: virtual reality training and learning curve," *Journal of the Society of Laparoendoscopic Surgeons Journal of the Society of Laparoendoscopic Surgeons*, vol. 18, no. 3, Article ID e2014.00258, 2014.
- [15] R. Nair, S. Vishwakarma, M. Soni, T. Patel, and S. Joshi, "Detection of COVID-19 cases through X-ray images using hybrid deep neural network," *World Journal of Engineering*, vol. 19, no. 1, pp. 33–39, 2021.
- [16] T. Sharma, R. Nair, and S. Gomathi, "Breast cancer image classification using transfer learning and convolutional neural network," *IJMORE*, vol. 2, no. 1, pp. 8–16, 2022
- [17] J. Kuruvilla and K. Gunavathi, "Lung cancer classification using neural networks for CT images," *Computer Methods and Programs in Biomedicine*, vol. 113, no. 1, pp. 202–209, 2014.
- [18] M. Nasser and S. S. Abu-Naser, "Lung cancer detection using artificial neural network," *International Journal of Engineering and*

- Information Systems (IJEAIS), vol. 3, no. 3, pp. 17–23, 2019.
- [19] S. Minaee, Y. Y. Boykov, F. Porikli, A. J. Plaza, N. Kehtarnavaz, and D. Terzopoulos, “Image segmentation using deep learning: a survey,” *IEEE Transactions on Pattern Analysis and Machine Intelligence*, p. 1, 2021.
- [20] G. Zhang, G. Kang, Y. Wei, and Y. Yang, “Few-shot segmentation via cycle-consistent transformer,” 2021, arXiv preprint arXiv:2106.02320.
- [21] H. Tang, X. Qi, D. Xu, P. H. Torr, and N. Sebe, “Edge guided GANs with semantic preserving for semantic image synthesis,” 2020, arXiv preprint arXiv:2003.13898.
- [22] S. M. Naqi, M. Sharif, and A. Jaffar, “Lung nodule detection and classification based on geometric fit in parametric form and deep learning,” *Neural Computing and Applications*, vol. 32, no. 9, pp. 4629–4647, 2020.
- [23] G. Savitha and P. Jidesh, “A holistic deep learning approach for identification and classification of sub-solid lung nodules in computed tomographic scans,” in *Computers & Electrical Engineering*, vol. 84, article 106626, Elsevier, New York, United States, 2020.
- [24] Lung Cancer Staging Essentials, available at <http://pubs.rsna.org/doi/full/10.1148/rq.305095166>
- [25] Shiyong Hu, Eric A Huffman, and Joseph M. Reinhardt, “Automatic lung segmentation for accurate quantitation of volumetric X-Ray CT images”, *IEEE Transactions on Medical Imaging*, vol. 20, no. 6 pp. 490–498, June 2001.
- [26] P. Soille, “Morphological Image Analysis - Principles and Applications”, Springer-Verlag, 1999.
- [27] Rathod, S., Ragha, L.: *Analysis of CT Scan Lung Cancer Images using Machine Learning Algorithms* (2022)

BIOGRAPHIES OF AUTHORS

	<p>Prof. Seema Babusing Rathod     has completed her B.E. in Computer Science Engineering from Prof. Ram Meghe Institute of Technology and Research, M. E in Information and Technology from Sipna College of engineering and Technology, Amravati and Ph.D pursuing in Computer Engineering from Lokmanya Tilak College of Engineering LTCE- Navi Mumbai. She had worked as a two-time Exam Controller and Exam valuer officer At Amravati university.</p>
	<p>Dr. Lata L. Ragha     has received her Ph. D. degree from Jadavpur University, Kolkata in 2011. She received her B. E. and M. Tech degree in Computer Science and Engineering from Karnatak University in 1987 and Vishveshwarai Technological University, Karnataka, in 2000 respectively. She is currently working as Professor and Head, Department of Computer Engineering at Fr. C. Rodrigues Institute of Technology, Vashi, Navi-Mumbai. Her research interests include Networking, Security, Internet Routing, and Data Mining. She has more than 160 research publications in International Journals and conferences</p>